Journal of Biomedical Optics

BiomedicalOptics.SPIEDigitalLibrary.org

Quantitative short-wave infrared multispectral imaging of *in vivo* tissue optical properties

Robert H. Wilson
Kyle P. Nadeau
Frank B. Jaworski
Rebecca Rowland
John Q. Nguyen
Christian Crouzet
Rolf B. Saager
Bernard Choi
Bruce J. Tromberg
Anthony J. Durkin

SPIE.

Journal of Biomedical Optics 19(8), 086011 (August 2014)

Quantitative short-wave infrared multispectral imaging of *in vivo* tissue optical properties

Robert H. Wilson,[a] Kyle P. Nadeau,[a] Frank B. Jaworski,[b] Rebecca Rowland,[a] John Q. Nguyen,[a] Christian Crouzet,[a] Rolf B. Saager,[a] Bernard Choi,[a] Bruce J. Tromberg,[a] and Anthony J. Durkin[a,*]
[a]University of California, Beckman Laser Institute, Irvine, 1002 Health Sciences Road, Irvine, California 92612, United States
[b]Raytheon Vision Systems, 75 Coromar Drive, Goleta, California 93117, United States

Abstract. Extending the wavelength range of spatial frequency domain imaging (SFDI) into the short-wave infrared (SWIR) has the potential to provide enhanced sensitivity to chromophores such as water and lipids that have prominent absorption features in the SWIR region. Here, we present, for the first time, a method combining SFDI with unstructured (zero spatial frequency) illumination to extract tissue absorption and scattering properties over a wavelength range (850 to 1800 nm) largely unexplored by previous tissue optics techniques. To obtain images over this wavelength range, we employ a SWIR camera in conjunction with an SFDI system. We use SFDI to obtain *in vivo* tissue reduced scattering coefficients at the wavelengths from 850 to 1050 nm, and then use unstructured wide-field illumination and an extrapolated power-law fit to this scattering spectrum to extract the absorption spectrum from 850 to 1800 nm. Our proof-of-principle experiment in a rat burn model illustrates that the combination of multispectral SWIR imaging, SFDI, and unstructured illumination can characterize *in vivo* changes in skin optical properties over a greatly expanded wavelength range. In the rat burn experiment, these changes (relative to normal, unburned skin) included increased absorption and increased scattering amplitude and slope, consistent with changes that we previously reported in the near-infrared using SFDI. [DOI: 10.1117/1.JBO.19.8.086011]

Keywords: wide-field optical imaging; short-wave infrared imaging; spatial frequency domain imaging; multispectral imaging; optical properties.

Paper 140250R received Apr. 24, 2014; revised manuscript received Jul. 17, 2014; accepted for publication Jul. 17, 2014; published online Aug. 13, 2014.

1 Introduction

Over the past two decades, optical methods have been widely employed to obtain information about the absorption and scattering content of biological tissues.[1] Recently, spatial frequency domain imaging (SFDI) has been developed to extract spatially resolved tissue properties at multiple wavelengths from reflectance measurements at multiple spatial frequencies.[2] SFDI studies have typically employed wavelengths in the near-infrared (NIR) (650 to 1000 nm).

Expanding the wavelength range of SFDI to include the short-wave infrared (SWIR) can potentially provide increased sensitivity to water[3] and lipids,[3,4] both of which have absorption features throughout the SWIR that are more prominent than those found in the NIR. Thus, SWIR imaging has the potential to complement NIR imaging approaches.[5]

SWIR optical sensing of skin has previously been employed to spectrally characterize porcine[6,7] and human[8,9] skin properties. However, these measurements have largely been performed on *ex-vivo* tissue samples using integrating sphere based techniques.[6–9]

In this letter, we report on integration of SFDI methods, which we have previously described elsewhere,[1,2,10] with planar illumination and a SWIR camera capable of spectral imaging from 850 to 1800 nm. This combination of SWIR instrumentation and a hybrid SFDI procedure (using data from both structured and uniform planar light) enables us to obtain tissue absorption and scattering spectra well into the SWIR wavelength range.

2 Experimental Methods

The outline of this hybrid SFDI technique is as follows: (1) SFDI data from 850 to 1050 nm is employed to extract the tissue reduced scattering coefficient using a Monte Carlo fitting method. (2) The reduced scattering coefficients are fit with a power law to extrapolate the scattering spectrum at SWIR wavelengths. (3) The reflectance data from unstructured illumination and the extrapolated scattering spectrum are employed to solve for the absorption spectrum over the entire wavelength range. The hybrid SFDI method can extract tissue optical properties over a greatly expanded wavelength range (850 to 1800 nm) that has not been heavily explored by SFDI or other tissue optics methods.

Here, for a proof-of-principle experiment, we employed this hybrid SFDI procedure to characterize SWIR tissue optical properties in an *in vivo* rat model of partial-thickness burns. Following the controlled rat burn protocol, detailed in Nguyen et al. [10], partial thickness burns were produced on the lateral side of a shaved 500 g Sprague–Dawley rat using a brass burn comb heated to 100°C. The comb was placed in contact with the skin for 8 s, producing four deep partial thickness burn areas, 1×2 cm^2 in size. Upon conclusion of the experiment, the burn areas were resected and prepared for histological examination. This *in vivo* preclinical work was approved by the Animal Care and Use Committee at University of California, Irvine (#1999-2064).

*Address all correspondence to: Anthony J. Durkin, E-mail: adurkin@uci.edu

The imaging setup for the rat burn measurements is similar to that employed previously,[10] except with a SWIR camera for detection. The sample was illuminated with multiple spatially modulated patterns of broadband light from a tungsten halogen lamp projected through a digital micromirror device (DMD, Texas Instruments, Dallas, Texas).[2] A Raytheon Vision Systems minSWIR camera was employed to detect reflectance over 850 to 1800 nm. The camera contained an InGaAs detector array and a SB373 CMOS readout, and the lens was attached to a Perkin-Elmer (Waltham, Massachusetts) liquid crystal tunable filter (#131928 LNIR 850 to 1800 nm, FWHM = 6 nm at 850 nm, FWHM = 32 nm at 1790 nm). The camera integration time was set to 32 ms. Images were acquired preburn and ~2 h postburn. At both time points, the data consisted of reflectance images taken in 50 nm steps from 850 to 1800 nm, using three spatial frequencies: 0, 0.05 mm^{-1}, and 0.10 mm^{-1}. A solution of 2% Intralipid[9] was used as a reference phantom.

3 Data Analysis Methods and Results

With the hybrid SFDI method, we can use both efficiently transmitted unstructured light in the SWIR range and spatially modulated wavelengths in the NIR to extract the absorption coefficient (μ_a) and reduced scattering coefficient (μ_s') spectra over the entire 850 to 1800 nm range. First, spatially resolved maps of μ_a and μ_s' were obtained at the five shortest wavelengths (850, 900, 950, 1000, and 1050 nm) by fitting the spatial frequency-dependent reflectance images pixel-by-pixel to a Monte Carlo model[10] of light transport. The extracted μ_s' maps at the aforementioned five wavelengths were fit with a power-law model: $\mu_s'(\lambda) = A(\lambda/\lambda_o)^{-b}$, where λ is the wavelength of the light and λ_o is a "reference" wavelength (set here to 850 nm). This power law is a well-known approximation for bulk tissue scattering[11–13] and has previously been shown (via comparison with integrating sphere data) to be an accurate model for the scattering coefficient of biological tissue over the 850- to 1800-nm wavelength range.[8,9] This procedure produced spatial maps of the reduced scattering amplitude A and slope b.

Second, a power law was employed to extrapolate the reduced scattering spectrum over the 1100 to 1800 nm range.[12] This method has been extensively employed in the time/frequency domain for diffuse optical spectroscopy "point-measurement" studies of breast and skin.[12,13] Here, we have extended the approach to SFDI. The mean μ_s' spectra over a region of interest were calculated for the rat tissue preburn and postburn (Fig. 1). Over this region of interest, the (mean ± standard deviation) value of the reduced scattering amplitude was calculated to be $A = 1.33 \pm 0.02$ prior to the burn and $A = 1.55 \pm 0.01$ at ~2 h postburn, while the value of the reduced scattering slope was calculated to be $b = 0.61 \pm 0.02$ prior to the burn and $b = 0.68 \pm 0.01$ at ~2 h postburn. This result suggests that the scattering parameters A and b have the potential to distinguish between burned and nonburned tissues as we have seen in our NIR rat burn studies.[10]

Finally, the extrapolated μ_s' values were employed to extract the μ_a maps from the unstructured illumination reflectance images.[12] The extracted scattering amplitude A and absorption coefficient μ_a obtained by this hybrid SFDI method at 1350 nm are shown in Fig. 2 for rat tissue preburn and ~2 h postburn. We use 1350 nm as a representative example of an SWIR wavelength at which water absorption is notably (~5×) greater than at the 970 nm NIR absorption peak.[14] The mean preburn and postburn SWIR μ_a spectra over the region of interest denoted by the white box in Fig. 2 are shown in Fig. 3. As Fig. 3 suggests, many of the detected SWIR wavelengths (especially those in the 1100 to 1600 nm range) have the potential to

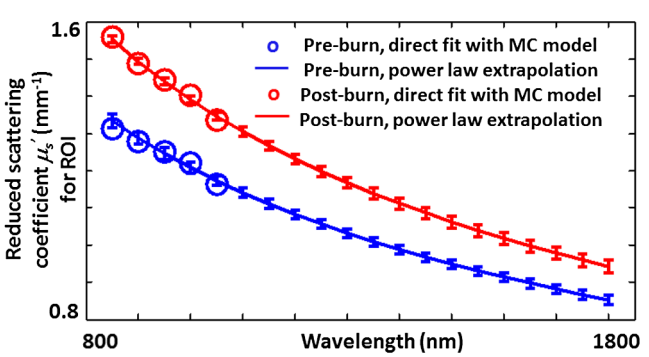

Fig. 1 Reduced scattering spectra of rat tissue preburn (blue) and postburn (red), with extrapolated (850 to 1800 nm) power-law reduced scattering spectra (solid curves) plotted alongside reduced scattering coefficient values obtained directly by pixel-by-pixel fitting (circles) with a Monte Carlo model for the wavelengths from 850 to 1050 nm. The error bars represent the standard deviation of the extrapolated reduced scattering coefficient over the region of interest. The error bars for the direct-fit scattering coefficient are not pictured, as they are within the diameter of the circles.

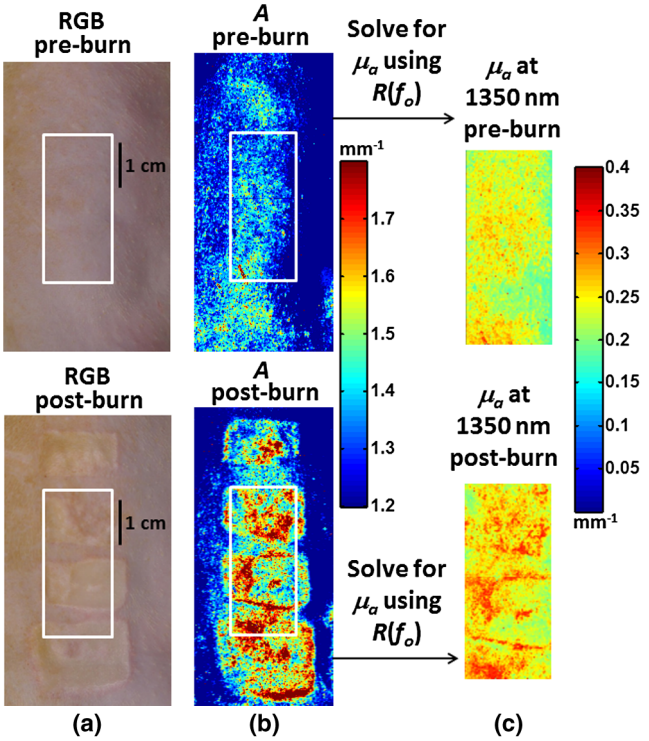

Fig. 2 (a) Digital color images (preburn and ~2 h postburn) of the region of the rat that was contacted with the burn comb. (b) Map of reduced scattering amplitude A (preburn and ~2 h postburn), from extrapolated power-law fit to reduced scattering coefficient obtained with SFDI from 850 to 1050 nm, over the region of the rat that was contacted with the burn comb. (c) Map of absorption coefficients at 1350 nm (preburn and ~2 h postburn), over the subregion denoted by the white box in the color images and scattering amplitude maps, obtained by using the extrapolated reduced scattering coefficient and the unstructured illumination reflectance data $R(f_0)$ at 1350 nm.

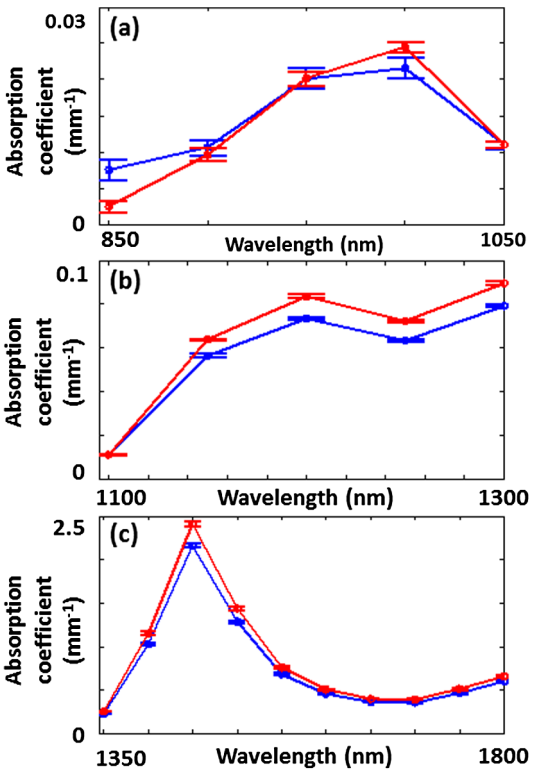

Fig. 3 (a) Mean extracted absorption coefficients from 850 to 1050 nm for rat tissue preburn (blue) and ~2 h postburn (red) for the region of interest shown in Fig. 2. (b) Same as (a) but for 1100 to 1300 nm. (c) Same as (a) and (b) but for 1350 to 1800 nm. For all three panels, the error bars represent the standard deviation of the absorption coefficient over the region of interest.

provide μ_a maps that may provide insight into tissue functional status, such as changes in hydration/edema, as suggested by Fig. 2. For instance, we report an absorption coefficient (attributed primarily to water in the SWIR regime) of normal rat tissue that is 3.4× greater at 1200 nm [Fig. 3(b)] than at 1000 nm [Fig. 3(a)] and 100× greater at 1450 nm [Fig. 3(c)] than at 1000 nm.

The multispectral SWIR data illustrate a mean postburn increase of greater than 10% in μ_a over the 1150 to 1800 nm range. This change is attributed to increased water fraction caused by edema, as previously observed in partial-thickness burns using SFDI in the NIR regime.[10] The SWIR data also show a postburn decrease in μ_a from 850 to 900 nm, a postburn increase of 16% in the reduced scattering amplitude, and a postburn increase of 11% in the reduced scattering slope. Similar burn-related trends in absorption and reduced scattering slope were observed in Ref. 10, attributed to changes in hemoglobin content and denaturation of collagen, respectively.

4 Discussion and Conclusions

This proof-of-principle experiment was constrained by several factors. First, at many wavelengths greater than 1050 nm that are associated with water absorption, the signal-to-noise ratio of the collected reflectance at spatial frequencies greater than $f_x = 0$ was insufficient to determine optical properties by direct fit. Second, the light engine, through which excitation from the source must pass in order to obtain structured illumination, is a source of significant transmission loss through the optical system. Third, the integration of the SWIR camera with the SFDI system was not optimized to maximize SNR for the entire wavelength range (due to proprietary software constraints related to the Raytheon SWIR camera). Future work will involve refinements to the light delivery and detection method over the entire 850 to 1800 nm range, to improve signal-to-noise and enhance precision in the SWIR reflectance and tissue optical property measurements.

In this study, we have combined an SFDI system with a SWIR camera that detects light from 850 to 1800 nm. This experiment serves as a proof of principle for two key concepts: (1) integration of SFDI with unstructured illumination and (2) use of this hybrid SFDI technique to measure tissue optical properties over an expanded wavelength range (850 to 1800 nm). As a specific biological example, we used the hybrid SFDI method to quantify *in vivo* burn related changes in the optical properties of rat skin over this wide wavelength range, which is not typically employed in SFDI experiments. The SWIR range provides two key advantages for enhanced tissue characterization: lower μ_s' relative to the NIR (enabling a ~20% increase in penetration depth at some wavelengths, such as 1100 nm, as compared to a typical penetration depth in the 650 to 1000 nm range[8]) and increased sensitivity to absorption from water and lipids.[15,16] These features of the SWIR regime also suggest potential for quantitative, noninvasive, wide-field burn severity analysis, which will be the topic of our future study.

Acknowledgments

R.H.W. was supported by a fellowship from the Hewitt Foundation for Medical Research. K.P.N. was supported by the NSF IGERT (Grant 1144901). F.B.J. was internally funded by Raytheon Vision Systems. Additional support is provided by the National Institutes of Health (NIH-R21EB014440 and NIH-R21NS078634), the NIH/NIBIB funded P41EB015890, the Military Medical Photonics Program (FA9550-10-1-0538), and the Arnold and Mabel Beckman Foundation.

References

1. T. D. O'Sullivan et al., "Diffuse optical imaging using spatially and temporally modulated light," *J. Biomed. Opt.* **17**(7), 071311 (2012).
2. D. J. Cuccia et al., "Quantitation and mapping of tissue optical properties using modulated imaging," *J. Biomed. Opt.* **14**(2), 024012 (2009).
3. R. Nachabé et al., "Estimation of lipid and water concentrations in scattering media with diffuse optical spectroscopy from 900 to 1600 nm," *J. Biomed. Opt.* **15**(3), 037015 (2010).
4. I. Bargigia et al., "Time-resolved diffuse optical spectroscopy up to 1700 nm by means of a time-gated InGaAs/InP single photon avalanche diode," *Appl. Spectrosc.* **66**(8), 944–950 (2012).
5. Q. Cao et al., "Multispectral imaging in the extended near-infrared window based on endogenous chromophores," *J. Biomed. Opt.* **18**(10), 101318 (2013).
6. E. Zamora-Rojas et al., "Optical properties of pig skin epidermis and dermis estimated with double integrating spheres measurements," *Innov. Food Sci. Emerging Technol.* **20**, 343–349 (2013).
7. Y. Du et al., "Optical properties of porcine skin dermis between 900 nm and 1500 nm," *Phys. Med. Biol.* **46**(1), 167–181 (2001).
8. A. Bashkatov et al., "Optical properties of human skin, subcutaneous and mucous tissues in the wavelength range from 400 to 2000 nm," *J. Phys. D* **38**(15), 2543–2555 (2005).
9. T. L. Troy and S. N. Thennadil, "Optical properties of human skin in the near infrared wavelength range of 1000 to 2200 nm," *J. Biomed. Opt.* **6**(2), 167–176 (2001).
10. J. Q. Nguyen et al., "Spatial frequency domain imaging of burn wounds in a preclinical model of graded burn severity," *J. Biomed. Opt.* **18**(6), 066010 (2013).

11. S. L. Jacques, "Origins of tissue properties in the UVA, visible, and NIR regions," in *Advances in Optical Imaging and Photon Migration*, R. R. Alfano and J. G. Fujimoto, Eds., TOPS 2, pp. 364–371, Optical Society of America, Washington, DC (1996).
12. F. Bevilacqua et al., "Broadband absorption spectroscopy in turbid media by combined frequency-domain and steady-state methods," *Appl. Opt.* **39**(34), 6498–6507 (2000).
13. S.-H. Tseng et al., "Chromophore concentrations, absorption and scattering properties of human skin in vivo," *Opt. Express* **17**(17), 14599–14617 (2009).
14. G. M. Hale and M. R. Querry, "Optical constants of water in the 200 nm to 200 μm wavelength region," *Appl. Opt.* **12**(3), 555–563 (1973).
15. E. M. Attas et al., "Near-IR spectroscopic imaging for skin hydration: the long and the short of it," *Biopolymers* **67**(2), 96–106 (2002).
16. R. Nachabe et al., "Estimation of biological chromophores using diffuse optical spectroscopy: benefit of extending the UV–VIS wavelength range to include 1000 to 1600 nm," *Biomed. Opt. Express* **1**(5), 1432–1442 (2010).

Biographies of the authors are not available.